



ARTICLE

Aescin-induced reactive oxygen species play a pro-survival role in human cancer cells via ATM/AMPK/ULK1-mediated autophagy

Bin Li¹, Guo-liang Wu¹, Wei Dai¹, Gang Wang¹, Hao-yuan Su¹, Xue-ping Shen¹, Rui Zhan¹, Jia-ming Xie², Zhong Wang², Zheng-hong Qin³, Quan-gen Gao¹ and Gen-hai Shen¹

Aescin, a natural mixture of triterpene saponins, has been reported to exert anticancer effect. Recent studies show that aescin increases intracellular reactive oxygen species (ROS) levels. However, whether the increased ROS play a role in the anticancer action of aescin remains to be explored. In this study, we demonstrated that aescin (20–80 µg/mL) dose-dependently induced apoptosis and activated mammalian target of rapamycin (mTOR)-independent autophagy in human hepatocellular carcinoma HepG2 cells and colon carcinoma HCT 116 cells. The activation of autophagy favored cancer cell survival in response to aescin, as suppression of autophagy with ATG5 siRNAs or 3-methyladenine (3-MA), a selective inhibitor of autophagy, promoted aescin-induced apoptosis in vitro, and significantly enhanced the anticancer effect of aescin in vivo. Meanwhile, aescin dose-dependently elevated intracellular ROS levels and activated Ataxia-telangiectasia mutated kinase/AMP-activated protein kinase/UNC-51-like kinase-1 (ATM/AMPK/ULK1) pathway. The ROS and ATM/AMPK/ULK1 pathway were upstream modulators of the aescin-induced autophagy, as *N*-acetyl-L-cysteine (NAC) or ATM kinase inhibitor (KU-55933) remarkably suppressed aescin-induced autophagy and consequently promoted aescin-induced apoptosis, whereas overexpression of ATG5 partly attenuated NAC-induced enhancement in aescin-induced apoptosis. In conclusion, this study provides new insights into the roles of aescin-mediated oxidative stress and autophagy in cancer cell survival. Our results suggest that combined administration of the antioxidants or autophagic inhibitors with aescin might be a potential strategy to enhance the anticancer effect of aescin.

Keywords: aescin; ROS; autophagy; apoptosis; human hepatocellular carcinoma HepG2 cells; human colon carcinoma HCT 116 cells; 3-MA; NAC; KU-55933.

Acta Pharmacologica Sinica (2018) 39:1874–1884; <https://doi.org/10.1038/s41401-018-0047-1>

INTRODUCTION

Reactive oxygen species (ROS) serve as essential signaling transducers that mediate numerous physiological and pathophysiological processes [1]. Increased ROS levels have been implicated in cancer cell initiation, differentiation, angiogenesis, therapeutic resistance and autophagy via a wide variety of signaling pathways [2, 3]. However, excessive levels of ROS may be toxic to cancer cells and can potentially lead to cell senescence, cell cycle arrest and even cell death. Although the “double-edged-sword” property of ROS induces cancer cell survival or death depending on intracellular context and ROS levels, ROS-manipulation strategies may be potentially effective approaches in cancer therapies [3].

Macroautophagy, which is also referred to simply as autophagy, is a catabolic pathway to support metabolism and clear damaged proteins and organelles in response to insufficient nutrient supplies and other metabolic stress [4, 5]. Autophagy is stimulated by multiple forms of cellular stress, including ROS [6, 7]. The

mechanisms by which ROS regulate autophagy are complex. ROS stimulate autophagy via Jun-amino-terminal kinase (JNK1)/Bcl-2 pathway activation to release Beclin1 from the Bcl-2/Beclin1 complex [8] and via inhibition of the AKT/mammalian target of rapamycin (mTOR) pathway. Furthermore, ROS activate AMP-activated protein kinase/UNC-51-like kinase -1 (AMPK/ULK1) pathway to initiate autophagy and inactivate ATG4 to inhibit the delipidation of LC3, which results in the formation of autophagosomes [9, 10]. Indeed, the selective degradation of catalase by autophagy can provide a positive feedback loop that increases ROS and autophagy. Conversely, the autophagic degradation of mitochondria or other damaged organelles alleviates oxidative stress progression and acts as a negative feedback loop [7, 9]. In addition, ataxia-telangiectasia mutated kinase (ATM) is also implicated in metabolic pathways [11] and oxidative stress [12]. Activation of ATM by ROS can trigger AMPK and tuberous sclerosis complex 2 (TSC2), thus repressing the activity of mTORC1 and inducing autophagy [13, 14]. Moreover, AMPK promotes

¹Department of General Surgery, The First People's Hospital of Wu Jiang, Suzhou 215200, China; ²Department of General Surgery, Second Affiliated Hospital of Soochow University, Suzhou, 215004 Jiangsu, China and ³Department of Pharmacology and Laboratory of Aging and Nervous Diseases, Jiangsu Key Laboratory of Translational Research and Therapy for Neuro-Psycho-Diseases, Jiangsu Key Laboratory of Preventive and Translational Medicine for Geriatric Diseases, College of Pharmaceutical Science, Soochow University, Suzhou 215123, China

Correspondence: Z-h. Qin (qinzhonghong@suda.edu.cn) or Q-g. Gao (wjyqgg@sohu.com) or G-h. Shen (wjsgh3026@sina.com)

Received: 17 January 2018 Accepted: 20 May 2018

Published online: 19 June 2018

autophagy by directly activating ULK1 and Beclin1 phosphorylation under glucose starvation condition [15, 16]. Taking this evidence together, autophagy could be activated by ROS through multiple pathways.

Aescin or β -aescin, a natural mixture of triterpene saponins extracted from *Aesculus hippocastanum*, has demonstrated anti-inflammatory and anti-edema activities [17]. Recent studies have found that aescin can potentially inhibit tumor growth [18, 19], colonic aberrant crypt foci formation [18], and cancer cell proliferation as well as induce apoptosis in cancer cells [20, 21]. More importantly, aescin has been reported to elevate intracellular ROS levels, which results in mitochondrial perturbation that may be involved in aescin-induced apoptosis [19]. A recent study showed that aescin induces apoptosis and autophagy via the ROS/p38 MAPK (mitogen activated protein kinases) pathway in human osteosarcoma cells [22]. However, the roles of aescin-induced ROS in the autophagy and apoptosis of human hepatocellular carcinoma (HCC) cells and human colon carcinoma cells are still unclear.

In this study, we found that aescin increased ROS generation and activated the ATM/AMPK/ULK1 pathway, both of which were upstream molecules of aescin-induced protective autophagy. Suppression of autophagy markedly augmented aescin-induced apoptosis in vitro and enhanced the anticancer effect of aescin in vivo. Mechanistically, scavenging ROS and inhibiting the ATM pathway remarkably suppressed aescin-induced autophagy and concurrently aggravated aescin-induced apoptosis. This study expands our understanding of the roles of ROS and autophagy in the anticancer effect of aescin.

MATERIALS AND METHODS

Materials and reagents

Aescin was supplied by Shandong Luye Pharmaceutical Co., Ltd. (Yantai, China), dissolved in normal saline and diluted immediately prior to use. KU-55933 was purchased from Selleck Chemicals (S1092, Shanghai, China) and dissolved in dimethylsulfoxide (DMSO, DT0163, Shanghai, China). z-Val-Ala-Asp(OMe)-fluoromethylketone (Z-VAD-FMK) was purchased from Merck (Darmstadt, Germany) and dissolved in DMSO. Bafilomycin A1, 3-methyladenine (3-MA) and *N*-acetyl-L-cysteine (NAC) were purchased from Sigma-Aldrich (St Louis, MO, USA).

Cell culture

HCC HepG2 cells and human colorectal carcinoma (CRC) HCT 116 cells were obtained from the Chinese Academy of Sciences (Shanghai, China) and cultured with Dulbecco's modified Eagle's medium (GIBCO, USA) containing 10% fetal bovine serum (GIBCO, USA), 100 IU/mL penicillin and 100 IU/mL streptomycin in a humidified incubator at 37 °C under 5% CO₂ atmosphere. Cells were passaged at pre-confluent densities using 0.25% trypsin solution every 2 to 3 days. Cells were stored and used within 2 months after thawing of frozen aliquots.

ATG5 RNA interference and overexpression

To inhibit autophagy, *ATG5* siRNAs (GCAACUCUGGAUGG-GAUUGTT, *ATG5* siRNA1; CAUCUGAGCUACCCGGAUATT, *ATG5* siRNA2) were synthesized by GenePharma (Shanghai, China), and a scramble sequence (UUCUCCGAACGUGUCACGUTT) was synthesized as a negative control. HepG2 cells were plated in 6-well plates (500,000 cells/well) and cultured for 12 h. Cells were transfected with scramble small interfering RNA (siRNA) and *ATG5* siRNAs using LipofectamineTM RNAiMAX (Invitrogen, USA) with dilution in Opti-MEM Reduced Serum Medium (GIBCO, USA). The final concentration of scramble siRNA and *ATG5* siRNAs was 60 nM. Cells were cultured for 48 h and harvested for western blotting to detect the transfection efficiency or subjected to the following treatments.

The *ATG5* overexpression plasmid (Flag-*ATG5*) was kindly provided by Professor Wang Guanghui (College of Pharmaceutical Sciences, Soochow University, Suzhou, China). HepG2 cells were plated in 6-well plates (700,000 cells/well) and cultured for 12 h. Cells were transfected with Flag-NC and Flag-*ATG5* plasmids using Lipofectamine 3000 (Invitrogen, USA) with dilution in Opti-MEM Reduced Serum Medium (GIBCO, USA) for 36 h. The final concentration of Flag-NC and Flag-*ATG5* plasmids was 3 μ g/mL. Cells were cultured for 36 h and harvested for western blotting to detect the overexpression efficiency or subjected to the following treatments.

Western blotting analysis

Preparation of total protein lysates and western blotting analysis were performed as described previously [23]. The primary antibodies against p-ULK1 Ser317, ULK1, *ATG5*-*ATG12*, p-mTOR Ser2448, mTOR, Beclin1, p-AMPK Thr172, AMPK, poly (ADP-ribose) polymerase (PARP), caspase-9, cleaved-caspase-9, caspase-3 and cleaved-caspase-3 were from Cell Signaling Technology (CST, Danfoss, MA, USA). The anti-cleaved-caspase-3 antibody was also from ENZO Life Sciences (Farmingdale, NY, USA). The anti- β -actin antibody was from Sigma-Aldrich (St Louis, MO, USA). The LC3 antibody was from MBL (Nagoya, Japan), and antibodies against p-ATM Ser1981, ATM and GAPDH were from Abcam (Cambridge, UK). Secondary fluorescence antibodies (1:10,000; Jackson ImmunoResearch, anti-rabbit, 711-035-152, anti-mouse, 715-035-150) were used. Immunoreactivity was detected using an Odyssey Infrared Imager (Li-COR Biosciences).

HepG2 cell xenograft mouse model

HepG2 cells were infected with EGFP-LV-*ATG5*-shRNA lentivirus (*ATG5* #1: 5'-TTCATGGAATTGAGCCAAT-3'; *ATG5* #2: 5'-TTTCAT TCAGAAGCTGTTT-3' and *ATG5* #3: 5'-TGAACAGAAATCATCCTTAA-3'; multiplicity of infection (MOI) = 10; Shanghai GeneChem Co., Ltd., China) to inhibit the expression of *ATG5*. The expression level of *ATG5*-*ATG12* was successfully reduced. HepG2 cells and stable *ATG5* knockdown HepG2 cells (2×10^6) were subcutaneously inoculated into the left iliac fossa of 6-week-old female athymic nude mice (Shanghai SLAC Laboratory Animal Co. Ltd.). Tumor growth was measured twice a week using a caliper, and body weight was measured weekly. The tumor volume was calculated as follows: volume (mm³) = (length \times width²)/2. After the establishment of palpable tumors of 150–200 mm³, the tumor-bearing mice were assigned to five groups. Aescin (2 mg/kg) was then intraperitoneally injected into the mice every day for 12 days, while epirubicin (2 mg/kg), as a positive control, was intraperitoneally administered every 3 days for 12 days. Tumor sizes were measured every 3 days when aescin or epirubicin treatment was introduced. The mice were anesthetized and photographed. After the mice were killed, the tumors were dissected and photographed, and tumor proteins were extracted for western blotting analysis. All animal procedures were approved and monitored by the local Animal Care and Use Committee in Soochow University (Suzhou, China).

Flow cytometry (FCM) detection of ROS and apoptosis

FCM detection of ROS and apoptosis were performed as described previously [23]. HepG2 cells were treated with 0, 40, 60 or 80 μ g/mL aescin for 12 h or with 60 μ g/mL aescin for 0, 3, 6, 9, 12 or 18 h. ROS levels were determined using 2',7'-dichloro-dihydrofluorescein diacetate (H2-DCFDA, Beyotime Biotechnology, S0033, Shanghai, China) and quantified by FCM (FCMcan, Becton Dickinson). Assays were performed in triplicate and were repeated in three independent experiments.

Cell apoptosis was quantified with double staining for fluorescein isothiocyanate-conjugated Annexin-V and propidium iodide (Biouniquer, BU-AP0103). HepG2 cells were pretreated with

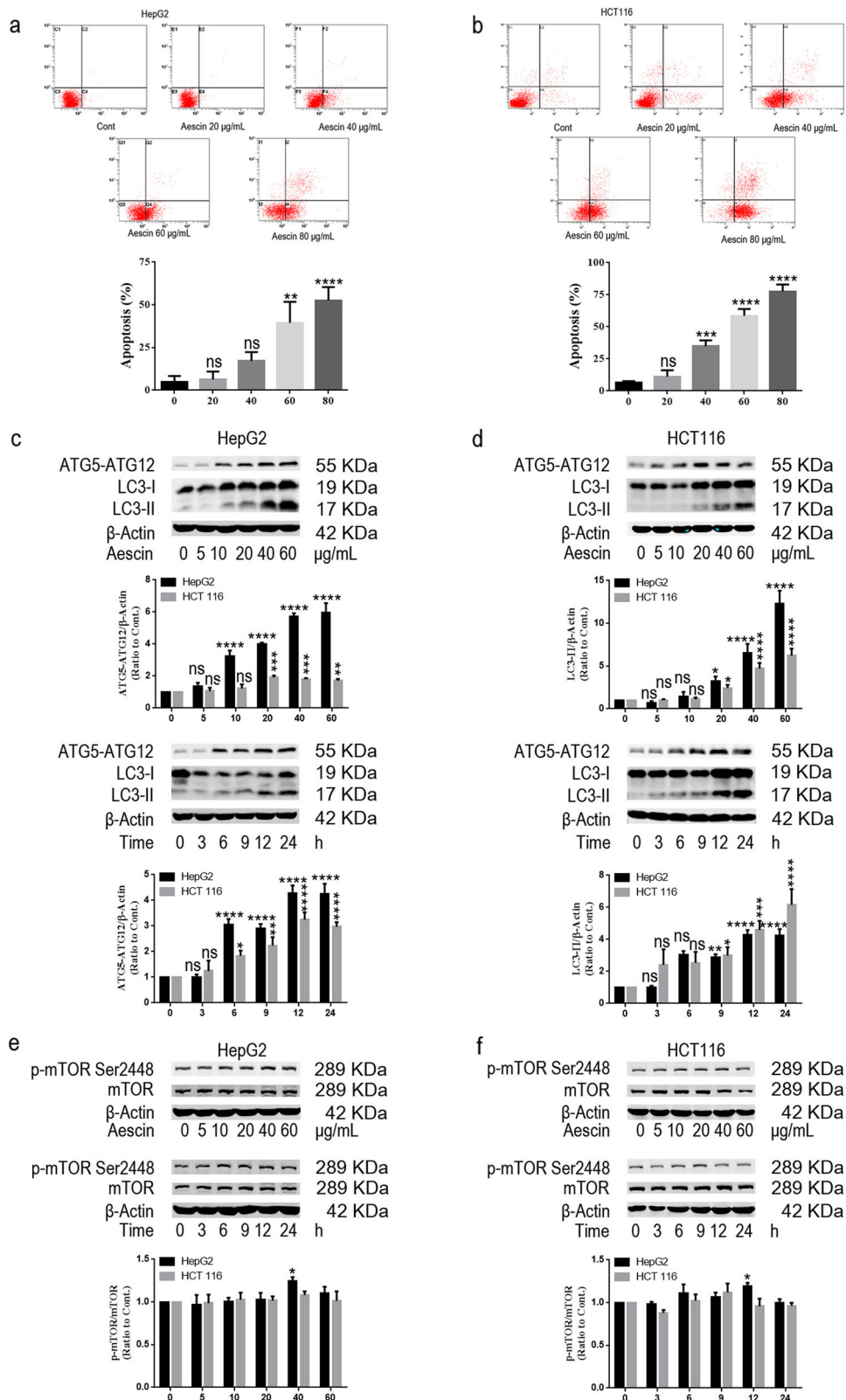


Fig. 1 Aescin induced apoptosis and activated autophagy in HepG2 and HCT 116 cells. **a, b** Aescin induced apoptosis in HepG2 and HCT 116 cells. Cells were treated with 0, 20, 40, 60 or 80 $\mu\text{g/mL}$ aescin for 12 h. The apoptosis of HepG2 cells (**a**) and HCT 116 cells (**b**) was determined by flow cytometry (FCM). The experiment was performed in three independent studies. Quantitative analysis of apoptosis was performed. **c, d** Aescin activated autophagy in HepG2 and HCT 116 cells. Cells were treated with 0, 5, 10, 20, 40 or 60 $\mu\text{g/mL}$ aescin for 12 h or treated with 40 $\mu\text{g/mL}$ aescin for 0, 3, 6, 9, 12 or 24 h. The protein expression levels were determined. **e, f** Aescin-activated autophagy was independent of the mTOR pathway. The expression levels of proteins were determined in HepG2 cells and HCT 116 cells. β -Actin was used as a loading control. Quantitative analysis was performed with ImageJ. The values are means \pm SD from three independent experiments. * $P < 0.05$; ** $P < 0.01$; *** $P < 0.001$; **** $P < 0.0001$; ns, $P > 0.05$ versus the control group

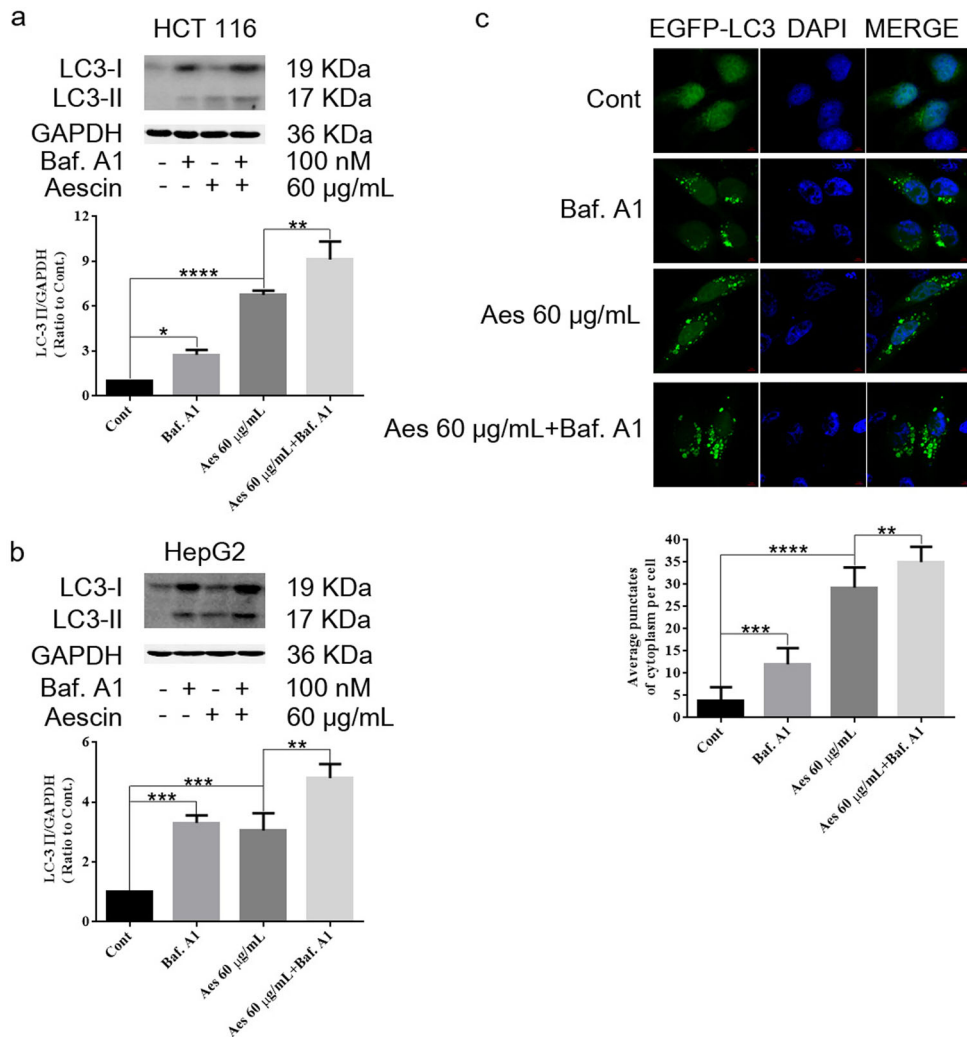


Fig. 2 Aescin regulated autophagic flux and promoted autophagosome biogenesis. **a, b** Aescin regulated autophagic flux in HepG2 and HCT 116 cells. Cells were treated with 60 µg/mL aescin and/or Bafilomycin A1 (Baf. A1, 100 nM) for 12 h. The protein expression levels were determined. GAPDH was used as a loading control. Quantitative analysis was performed with ImageJ. **c** Aescin promoted autophagosome biogenesis in HepG2 cells. Cells stably transfected with the EGFP-LC3 plasmid were treated with aescin and/or Baf. A1 (100 nM) for 12 h. Aescin-induced autophagy manifesting as EGFP-LC3 puncta was assessed using fluorescence microscopy. Quantitative analysis of EGFP-LC3 puncta was performed in various groups. The number of EGFP-LC3 puncta was counted in each cell of random fields. The percentage of EGFP-LC3 puncta-containing cells was assessed from 50 random fields. The values represent means ± SD from three independent experiments. * $P < 0.05$; ** $P < 0.01$; *** $P < 0.001$; **** $P < 0.0001$; ns, $P > 0.05$ versus the control group

NAC for 2 h before treatment with 0, 40, 60 and 80 µg/mL aescin for 12 h or treatment with 60 µg/mL aescin for 0, 6, 12 or 18 h. Freshly trypsinized cells were collected, washed twice with phosphate-buffered saline and processed following the manufacturer's instructions. A total of 10,000 cells per sample were acquired with an FCMcan flow cytometer. Cell fluorescence was analyzed by flow cytometry using the Cell Quest Pro software (Beckman Coulter).

EGFP-LC3 transient transfection

HepG2 cells were transfected with *ATG5* siRNA for 48 h or transfected with the EGFP-LC3 plasmid for 36 h using the LipofectamineTM RNAiMAX or Lipofectamine 3000 reagent (Invitrogen, USA), respectively. After transfection, the cells were pretreated with NAC for 2 h and then treated with 40 or 60 µg/mL aescin for 12 h. Before harvest, Bafilomycin A1 (100 nM) was added to cells for 4 h. Subsequently, the cells were observed with a Zeiss LSM710 confocal laser microscopy system and analyzed using the Zeiss LSM Browser.

Statistical analysis

Data were subjected to one-way analysis of variance using the GraphPad Prism 6 software statistical package (GraphPad Software, Inc., La Jolla, CA, USA). When a significant group effect was found, post hoc comparisons were performed using the Newman-Keuls *t*-test to examine special group differences. * $P < 0.05$; ** $P < 0.01$, *** $P < 0.001$ and **** $P < 0.0001$ were considered to be significant; ns, $P > 0.05$ versus corresponding group.

RESULTS

Aescin induced apoptosis and activated autophagy in HepG2 and HCT 116 cells

The anticancer effect of aescin on HepG2 and HCT 116 cells was investigated. As shown in Fig. 1a, b, aescin induced dose-dependent apoptosis in the two cell lines. When the cells were treated with 0, 20, 40, 60 or 80 µg/mL aescin for 12 h, the total apoptosis was 4.69% ± 3.65%, 6.34% ± 4.64%, 17.24% ± 5.13%, 39.47% ± 12.32% and 52.62% ± 7.79% in HepG2 cells and 6.74%

$\pm 1.00\%$, $11.14\% \pm 5.06\%$, $34.87\% \pm 4.54\%$, $58.71\% \pm 5.26\%$ and $77.71\% \pm 5.31\%$ in HCT 116 cells, respectively. In line with previous studies [20], aescin induced apoptosis in HepG2 and HCT 116 cells.

To investigate the protective responses in cancer cells in response to aescin, we evaluated the autophagy in aescin-treated HepG2 and HCT 116 cells. ATG5 and LC3 lipidation (LC3-

PE or LC3-II) are key markers of autophagy activation [24]. The level of ATG5-ATG12 was elevated when HepG2 and HCT 116 cells were treated with 20, 40 or 60 $\mu\text{g}/\text{mL}$ aescin for 12 h or with 40 $\mu\text{g}/\text{mL}$ aescin for 6, 9, 12 or 24 h (Fig. 1c, d). Furthermore, the level of LC3-II was significantly increased when HepG2 and HCT 116 cells were treated with 20, 40 or 60 $\mu\text{g}/\text{mL}$ aescin for 12 h or with 40 $\mu\text{g}/\text{mL}$

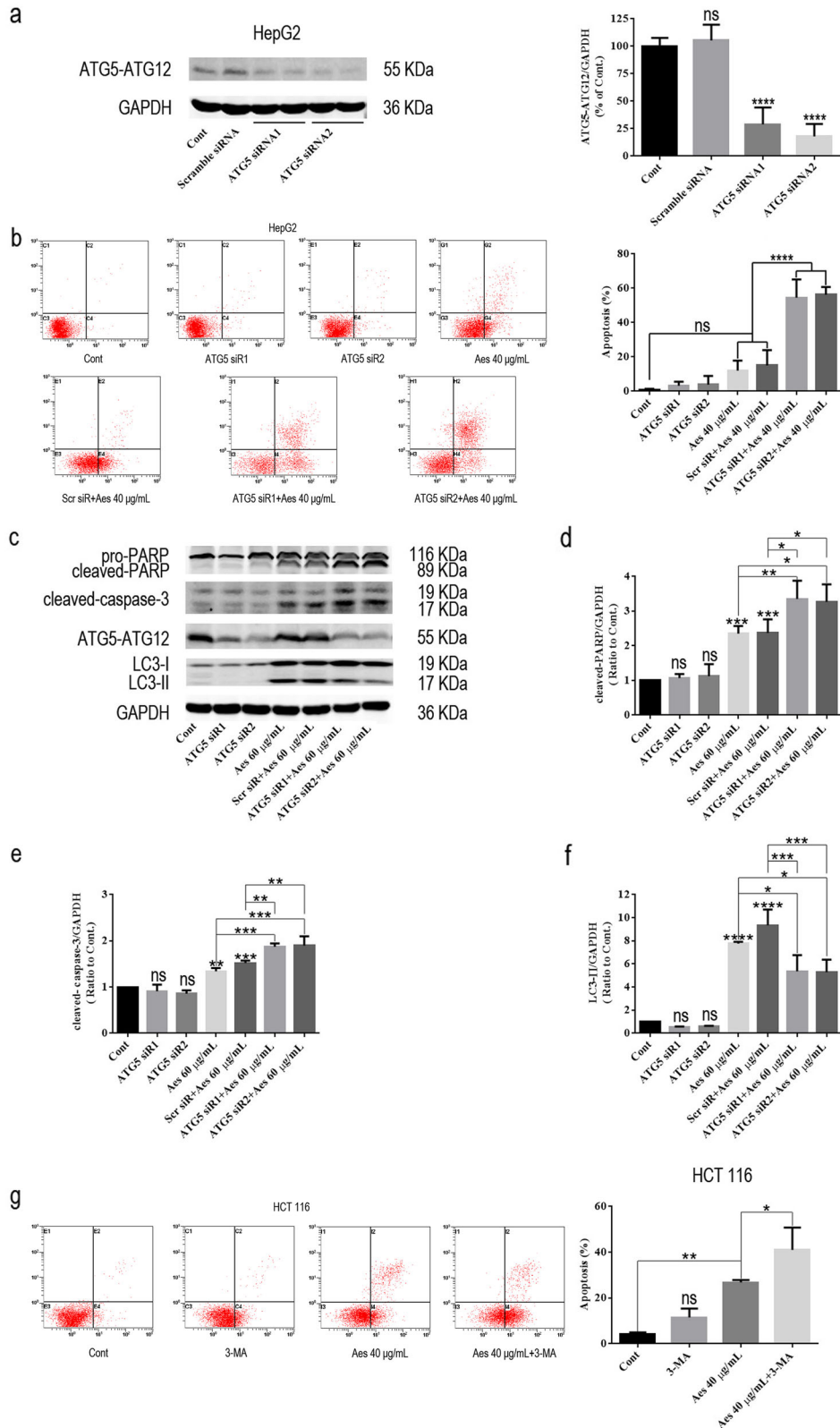


Fig. 3 Inhibition of autophagy by ATG5 knockdown aggravated aescin-induced apoptosis in vitro. **a** ATG5 knockdown in HepG2 cells. Cells were transiently transfected with scramble siRNA, *ATG5 siRNA1* or *ATG5 siRNA2* for 48 h. The level of ATG5-ATG12 was determined. **b-f** ATG5 knockdown increased aescin-induced apoptosis in HepG2 cells. Cells were transiently transfected with scramble siRNA or *ATG5 siRNA1/2* for 48 h and then were treated with or without 40 µg/mL aescin for 12 h. The apoptosis was measured by FCM. The experiment was performed in three independent studies. Quantitative analysis of apoptosis was performed (**b**). The protein expression levels were determined. GAPDH was used as a loading control (**c**). Quantitative analysis was performed with ImageJ (**d-f**). **g** 3-MA increased aescin-induced apoptosis in HCT 116 cells. Cells were pretreated with 3-MA (10 mM) for 12 h before treatment with or without 40 µg/mL aescin for 12 h. The apoptosis was measured by FCM. The experiment was performed in three independent studies. Quantitative apoptosis analysis was performed. The values are means ± SD from three independent experiments. **P* < 0.05; ***P* < 0.01; ****P* < 0.001; *****P* < 0.0001; ns, *P* > 0.05 versus the control group

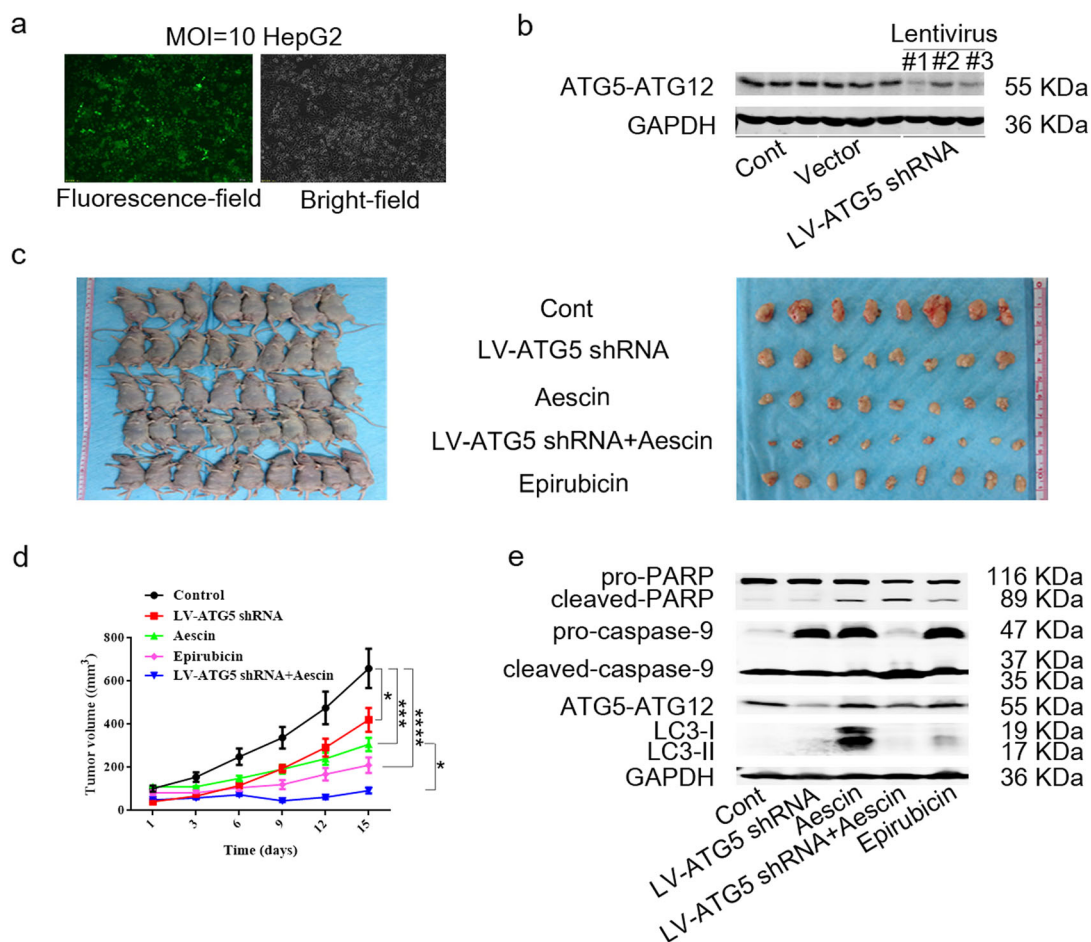


Fig. 4 Suppression of autophagy by ATG5 knockdown enhanced the anticancer effect of aescin in vivo. **a, b** ATG5 knockdown using lentivirus in HepG2 cells. Cells were infected with vector or EGFP-LV-ATG5-shRNA #1, #2 and #3 (MOI = 10). The EGFP-green fluorescence was verified by fluorescence microscopy (**a**). The protein expression levels were determined (**b**). **c** In vivo mouse tumor model. The different sizes of tumors were dissected from various groups of mice (*n* = 8 or 9). **d** Comparisons of tumor sizes between various groups. **e** The protein expression levels were determined in xenograft tumor tissues from various groups of mice. GAPDH was used as a loading control. **P* < 0.05; ****P* < 0.001; *****P* < 0.0001

aescin for 9, 12 or 24 h (Fig. 1c, d), indicating that aescin activated autophagy in dose- and time-dependent manners. Inhibition of the mTOR pathway is one of the main mechanisms by which autophagy is positively regulated. Consistent with inhibition of the mTOR pathway in autophagy-activated models, the level of p-mTOR Ser2448 was slightly increased in HepG2 cells treated with 40 µg/mL aescin for 12 h, whereas no significant change in HCT 116 cells was detected (Fig. 1e, f), suggesting that aescin-induced autophagy was independent of the mTOR pathway.

Aescin regulated autophagic flux and promoted autophagosome biogenesis

The augmentation of autophagosome markers, such as ULK1, ATG5 and LC3-II, could not distinguish between the increase

in autophagosome biogenesis and the decrease in autophagosome clearance [25]. To further discriminate between these two possibilities, we suppressed autophagosome-lysosome fusion using Bafilomycin A1 (Baf. A1). As shown in Fig. 2a, b, aescin or Baf. A1 increased the level of LC3-II in HepG2 and HCT 116 cells. More importantly, the elevated level of LC3-II was further increased in aescin- and Baf. A1-treated HepG2 and HCT 116 cells (Fig. 2a, b), suggesting apparent augmentation of autophagosome formation rather than reduced autophagosome clearance in response to aescin. To further confirm these findings, we transiently transfected cells with the EGFP-LC3 plasmid to detect green puncta reflective of autophagosome formation. In untreated cells, EGFP-LC3 was mostly located in the nucleus (Fig. 2c). However, in Baf. A1- or aescin-treated cells,

EGFP-LC3 mostly translocated from nucleus to cytoplasm and formed autophagosomes (green puncta) that mainly surrounded the nucleus (Fig. 2c). Notably, the elevated green

puncta were further augmented when the cells were treated with aescin and Baf. A1 (Fig. 2c), indicating that aescin regulated autophagic flux and promoted autophagosome biogenesis.

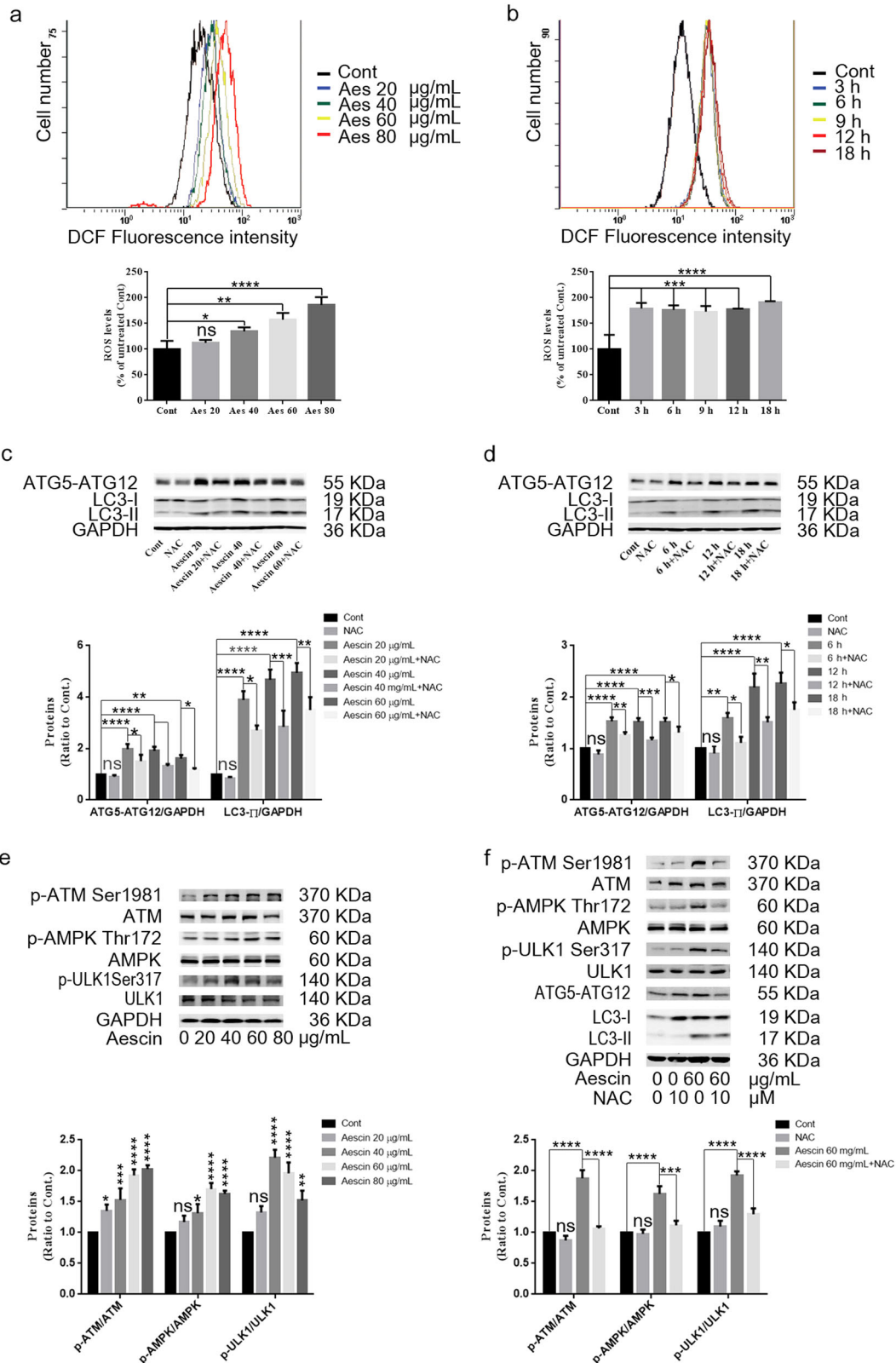


Fig. 5 Aescin-induced ROS activated the ATM/AMPK/ULK1 pathway and autophagy. **a, b** Aescin elevated ROS levels in HepG2 cells. Cells were treated with 0, 20, 40, 60 or 80 $\mu\text{g}/\text{mL}$ aescin for 12 h or with 60 $\mu\text{g}/\text{mL}$ aescin for 0, 3, 6, 9, 12 or 18 h. The ROS levels were measured by FCM. The experiment was performed in three independent studies. Quantitative analysis of ROS was performed. **c, d** NAC inhibited aescin-induced autophagy in HepG2 cells. Cells were pretreated with NAC (10 mM) for 2 h before being treated with 20, 40 and 60 $\mu\text{g}/\text{mL}$ aescin for 12 h or with 60 $\mu\text{g}/\text{mL}$ aescin for 6, 12 or 18 h. The protein expression levels were determined. **e** Aescin activated the ATM/AMPK/ULK1 pathway in HepG2 cells. Cells were treated as in (a). The protein expression levels were determined. **f** NAC suppressed aescin-activated ATM/AMPK/ULK1 pathway in HepG2 cells. Cells were pretreated with NAC for 2 h before being treated with 60 $\mu\text{g}/\text{mL}$ aescin for 12 h. The protein expression levels were determined. GAPDH was used as a loading control. Quantitative analysis was performed with ImageJ. The values are means \pm SD from three independent experiments. * $P < 0.05$; ** $P < 0.01$; *** $P < 0.001$; **** $P < 0.0001$; ns, $P > 0.05$ versus the control group

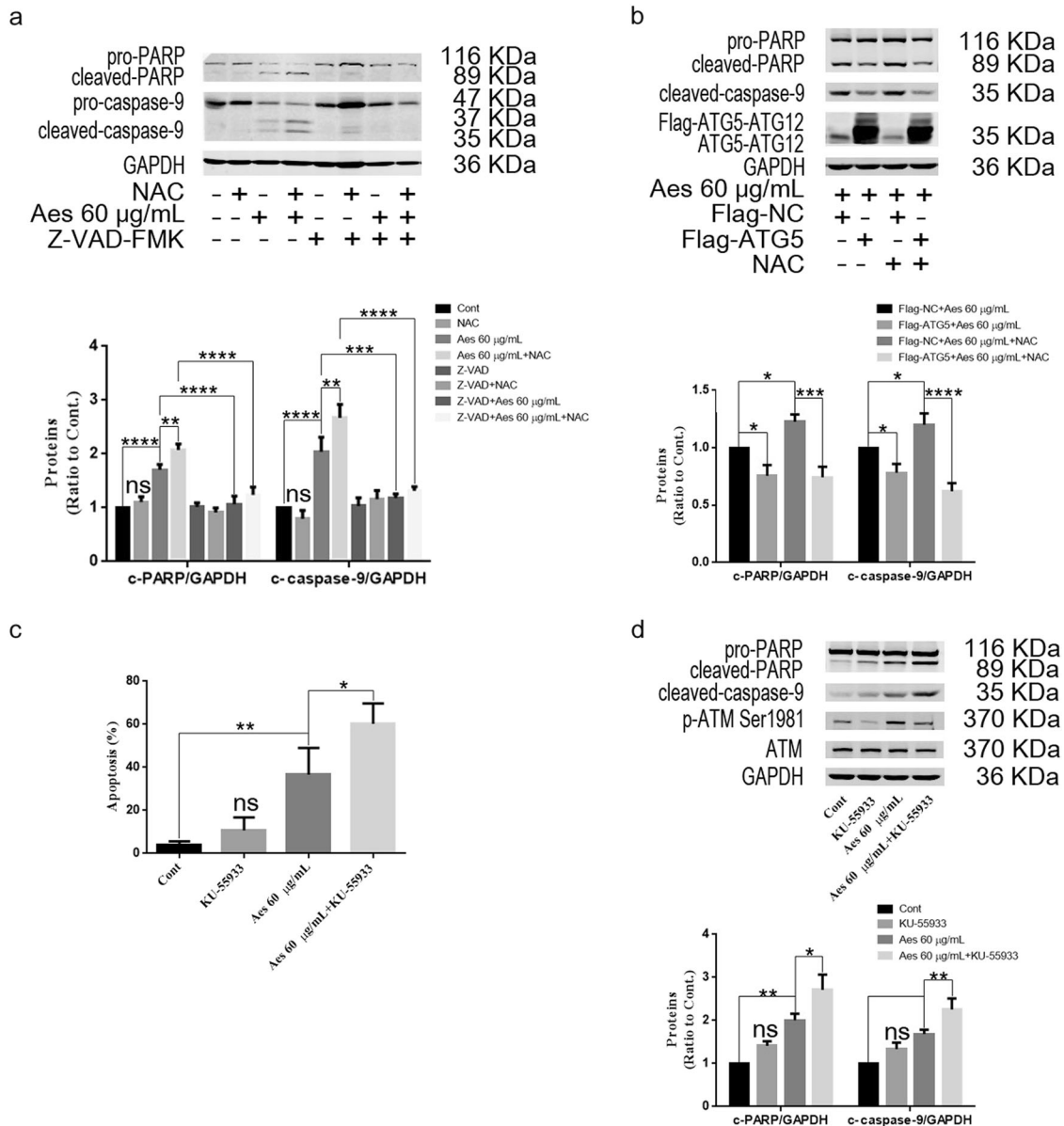


Fig. 6 NAC and ATM inhibitor augmented aescin-induced apoptosis, which was partly rescued by ATG5 overexpression. **a** Aescin induced caspase-dependent apoptosis in HepG2 cells. Cells were pretreated with NAC or Z-VAD-FMK (20 μM) for 2 h before being treated with 60 $\mu\text{g}/\text{mL}$ aescin for 12 h. The protein expression levels were determined. GAPDH was used as a loading control. Quantitative analysis of cleaved-PARP (c-PARP) and cleaved-caspase-9 (c-caspase-9) was performed with ImageJ. **b** Overexpression of ATG5 partly rescued aescin-induced apoptosis in HepG2 cells. Cells were transiently transfected with Flag-NC or Flag-ATG5 for 36 h and then pretreated with NAC for 2 h before being treated with 60 $\mu\text{g}/\text{mL}$ aescin for 12 h. The protein expression levels were determined. **c** ATM inhibitor increased aescin-induced apoptosis in HepG2 cells. Cells were pretreated with KU-55933 (10 mM) for 2 h before being treated with 60 $\mu\text{g}/\text{mL}$ aescin for 12 h. Apoptosis was measured by FCM. The experiment was performed in three independent studies. Quantitative analysis of apoptosis was performed. **d** The protein expression levels were determined. The values are means \pm SD from three independent experiments. * $P < 0.05$; ** $P < 0.01$; *** $P < 0.001$; **** $P < 0.0001$; ns, $P > 0.05$ versus the control group

Inhibition of autophagy enhanced aescin-mediated anticancer activity in vitro and in vivo

As autophagy can play pro-death or pro-survival roles in cancer cells [23, 26], we next explored the role of aescin-induced autophagy in aescin-mediated apoptosis. We successfully knocked down the expression of ATG5 using RNA interference, as the results showed that the level of ATG5-ATG12 was significantly decreased following transfection of HepG2 cells with *ATG5 siRNA1* and *ATG5 siRNA2* (Fig. 3a). More importantly, ATG5 knockdown markedly increased aescin-induced apoptosis (Fig. 3b). Moreover, the levels of cleaved-PARP and cleaved-caspase-3 were further increased in ATG5 knockdown and aescin-treated cells compared with aescin-treated and/or scramble siRNA-transfected cells (Fig. 3c–e). In addition, the autophagy activity was decreased by ATG5 knockdown in response to aescin (Fig. 3f). 3-MA, an inhibitor of autophagy due to suppression of class III PtdIns3K [27], was used to inhibit autophagy in HCT 116 cells. Similar to the results in HepG2 cells, inhibition of autophagy using 3-MA further increased aescin-induced apoptosis in HCT 116 cells (Fig. 3g). These results demonstrated that inhibition of aescin-induced autophagy aggravated aescin-induced apoptosis in vitro.

To further explore the function of autophagy in the anticancer effect of aescin in vivo, HepG2 cells were infected with lentivirus containing EGFP-LV-ATG5-shRNAs (#1, #2 and #3; MOI = 10) to suppress autophagy. The efficiency of lentiviral infection was determined by fluorescence detection in HepG2 cells (Fig. 4a). The expression level of ATG5-ATG12 was decreased when HepG2 cells were infected with lentivirus #1 or #3 (Fig. 4b). Therefore, lentivirus #3 was used to perform the following studies. As shown in Fig. 4c, d, ATG5 knockdown or aescin administration alone inhibited the growth of xenograft tumors. Notably, ATG5 knockdown remarkably augmented the anticancer effect of aescin compared with aescin or epirubicin (as a positive control) administration alone (Fig. 4c, d). Western blotting analysis of tumor tissue lysates revealed that the levels of ATG5-ATG12 and LC3-II were significantly decreased in tumor xenografts when the cells were infected with lentivirus #3 (Fig. 4e). However, the levels of cleaved-PARP and cleaved-caspase-9 were higher in the ATG5 knockdown and aescin-treated tissues than other tissues (Fig. 4e). We also observed the anticancer effect of epirubicin (Fig. 4c, d), as shown in our previous study [23]. These results were consistent with our in vitro studies, providing further evidence that downregulation of ATG5 and suppression of autophagy potentiates the anticancer activity of aescin in vitro and in vivo.

Aescin-induced ROS activated the ATM/AMPK/ULK1 pathway and autophagy

Aescin triggers intracellular ROS generation [19, 28]; however, whether aescin-induced ROS are implicated in aescin-induced autophagy and cell death is unknown. The ATM/AMPK/ULK1 pathway is involved in oxidative stress and the activation of autophagy [13, 14]. The present study found that aescin elevated the levels of ROS in HepG2 cells treated with 40, 60 or 80 µg/mL aescin for 12 h (Fig. 5a) or with 60 µg/mL aescin for 3, 6, 9, 12 or 18 h (Fig. 5b). NAC, a scavenger of ROS, eliminated aescin-induced ROS and remarkably suppressed the elevation of ATG5-ATG12 and LC3-II in HepG2 cells treated with 20, 40 or 60 µg/mL aescin for 12 h or with 60 µg/mL aescin for 6, 12 or 18 h (Fig. 5c, d), indicating that aescin-induced ROS were upstream signaling molecules of aescin-induced autophagy. Next, we detected the signaling pathway alterations in aescin-treated HepG2 cells. As shown in Fig. 5e, aescin activated the ATM/AMPK/ULK1 pathway, as the levels of p-ATM Ser1981, p-AMPK Thr172 and p-ULK1 Ser317 were significantly increased in HepG2 cells treated with 40, 60 or 80 µg/mL aescin for 12 h. We next determined the relationship between ROS and the ATM/AMPK/ULK1 pathway. As shown in Fig. 5f, NAC markedly decreased the levels of p-ATM Ser1981, p-AMPK Thr172 and p-ULK1 Ser317 in response to aescin

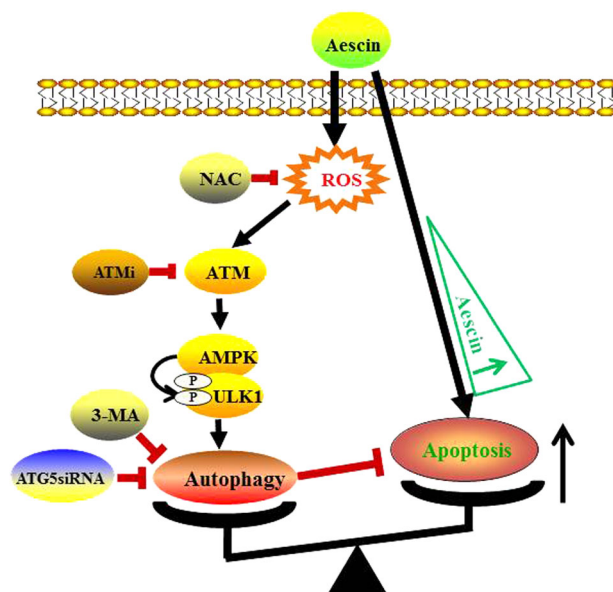


Fig. 7 Working model for aescin-induced oxidative stress, autophagy and apoptosis. Aescin-induced oxidative stress activated ATM/AMPK/ULK1 signaling node to induce protective autophagy. High concentration of aescin concurrently led to apoptosis. There is an interaction between aescin-induced autophagy and apoptosis. Suppression of aescin-induced autophagy consequently broke this balance and deteriorated aescin-induced apoptosis

compared with aescin treatment alone. These results showed that aescin-induced ROS activated the ATM/AMPK/ULK1 pathway, which plays an important role in autophagy activation.

Scavenging ROS and inhibiting the ATM pathway suppressed aescin-induced autophagy and augmented aescin-induced apoptosis

Caspase activation plays a crucial role in mitochondria-induced apoptosis. We next analyzed whether aescin-induced apoptosis is dependent on caspase activation. Z-VAD-FMK (Z-VAD), a pan-caspase inhibitor, was used to inhibit caspase activation. Compared with control and NAC-treated HepG2 cells, aescin alone mildly increased the levels of cleaved-PARP and cleaved-caspase-9, but the levels of these proteins were further elevated by NAC in response to aescin in HepG2 cells (Fig. 6a). However, the elevated levels of these proteins were significantly decreased following treatment with Z-VAD (Fig. 6a), suggesting that aescin-induced apoptosis was dependent on caspase activation.

Next, we explored whether overexpression of ATG5 could rescue NAC-increased apoptosis in response to aescin. As shown in Fig. 6b, overexpression of ATG5 slightly decreased the levels of cleaved-PARP and cleaved-caspase-9, indicating the protective function of ATG5 in response to aescin. Noticeably, overexpression of ATG5 significantly decreased the levels of these proteins, which were elevated by NAC and aescin in HepG2 cells, suggesting that ATG5 partly neutralized the function of NAC in the inhibition of autophagy and functionally rescued aescin-induced apoptosis.

To further investigate the role of the ATM pathway in aescin-induced apoptosis, KU-55933, an ATM inhibitor, was administered to inhibit ATM activation. Apparently, inhibition of ATM with KU-55933 further aggravated aescin-induced apoptosis (Fig. 6c). Moreover, the levels of cleaved-PARP and cleaved-caspase-9 were further increased by KU-55933 in response to aescin in HepG2 cells (Fig. 6d). These results demonstrated that inhibiting the ROS/ATM pathway suppressed aescin-induced autophagy and further aggravated aescin-induced apoptosis, which was partially rescued by overexpression of ATG5.

DISCUSSION

In this study, we determined the roles of ROS and autophagy in regulating aescin-induced apoptosis and found that aescin-induced ROS increased autophagy activity in cancer cells. NAC, an ATM kinase inhibitor, 3-MA and ATG5 knockdown all suppressed aescin-induced autophagy and aggravated aescin-induced apoptosis (Fig. 7). Mechanistically, aescin-induced ROS activated the ATM/AMPK/ULK1 signaling pathway to promote autophagy, which partly protected cancer cells against aescin-induced apoptosis (Fig. 7). Therefore, these data may highlight the therapeutic potential of aescin in combination with antioxidants and autophagy inhibitors in the treatment of cancer.

Cancer cells confer higher rates of ROS production and higher levels of antioxidant proteins than do normal cells to maintain redox homeostasis. As the amount of ROS exceeds the capacity of the antioxidant systems, oxidative stress occurs, followed by autophagy, which detoxifies ROS and relieves oxidative stress [29]. Therefore, treatment strategies will be ideally selected based on decreasing the beneficial ROS signaling and/or increasing the toxic ROS signaling [30]. In contrast to the antioxidative effects of aescin in nontumor cells [31], in the present study, aescin induced robust elevation of ROS in cancer cells (Fig. 5a, b) accompanied by activation of autophagy and induction of apoptosis (Fig. 1). Our question is whether aescin-induced ROS play a pro-survival or pro-death role in cancer cells.

In the present study, aescin notably stimulated ROS generation and autophagy activation to protect cancer cells from severe damage and apoptosis (Figs. 1 and 5), whereas repression of autophagy reversed the protective effect and decreased aescin-induced apoptosis (Figs. 3 and 6). Consistent with previous studies [20, 32], we also found that aescin alone exerted an anticancer effect *in vivo* (Fig. 4) and, more importantly, this effect was further enhanced when aescin-induced autophagy was suppressed *in vivo*. In addition, a recent study showed that aescin activates the ROS/p38 MAPK pathway and autophagy, which promotes aescin-induced apoptosis in osteosarcoma cells [22]. NAC or the autophagy inhibitor 3-MA decreases aescin-induced apoptosis in osteosarcoma cells [22]. This study showed that ROS and autophagy played a pro-survival function in HepG2 and HCT 116 cells. The reasons for the different results in the two models may be complicated. The doses and times of exposure to aescin, NAC and 3-MA are different. More importantly, the difference in tissue origin and malignant phenotype between osteosarcoma and HCC or CRC may account for the various responses to aescin, which suggests that aescin may be exerting an antitumor effect via different signaling pathways and mechanisms in various contexts.

The crosstalk between ROS-induced autophagy and apoptosis makes the potential translational implications more complicated. Combining aescin and autophagy-inhibiting agents can generate synergistic tumor killing activity (Fig. 3f) in the present models. Increasing studies consistently demonstrate that ROS are involved in upstream signaling to induce protective autophagy and that NAC diminishes the protective autophagy and augments apoptosis [33], as shown in this study (Fig. 6). Aescin-induced ROS activated the ATM/AMPK/ULK1 pathway to promote autophagy (Fig. 5), but that was independent of the mTORC1 pathway (Fig. 1). Furthermore, inhibition of ATM activity repressed aescin-induced autophagy and concurrently increased aescin-induced apoptosis (Fig. 6).

Noticeably, the central molecular modulators in the crosstalk between autophagy and apoptosis have been identified and include Bcl-2/Bcl-XL and certain autophagy proteins such as Beclin1, ATG5 and ATG4 [9]. The present study found that ATG5 may be the molecular modulator in the crosstalk between aescin-induced autophagy and apoptosis. Aescin upregulated ATG5 to activate autophagy and inhibit cancer cell apoptosis, whereas NAC downregulated ATG5 and induced caspase-dependent apoptosis

(Figs. 5 and 6). Conversely, ATG5 overexpression apparently rescued aescin-induced apoptosis, providing further evidence that ROS-induced autophagy exerted protective effects and facilitated cancer cell survival in response to aescin.

In conclusion, our study demonstrated that aescin-induced ROS promoted autophagy by activating the ATM/AMPK/ULK1 pathway. Scavenging ROS and suppressing autophagy effectively enhanced aescin's anticancer activity *in vitro* and *in vivo*. This study expands our understanding of the role of ROS in cancer cell survival and suggests a possible strategy of combining aescin with antioxidants or autophagic inhibitors in cancer therapy. However, the mechanisms by which aescin elevates intracellular ROS levels via increasing the rate of ROS production or decreasing the antioxidant systems should be further studied.

ACKNOWLEDGEMENTS

This work was supported by grants from the Jiangsu Provincial Commission of Health and Family Planning (No. YG201402, YG201503), Jiangsu Provincial Medical Youth Talent, (No. QNRC2016249), Suzhou Science and Technology Bureau (No. SYS2013041, SYS2016044, SYS2017041 and SYS201788), Wujiang District Science and Technology Bureau (No. WS201301), Wujiang District Commission of Health and Family Planning (No. WWK201607 and WWK201609) and National Natural Science Foundation of China (No. 81602613).

AUTHOR CONTRIBUTIONS

BL, Z-hQ, G-hS and Q-gG designed the research; BL, ZW, WD and G-IW performed the research; H-yS, X-pS and RZ contributed new reagents or analytic tools; J-mX and ZW analyzed the data; and BL and Z-hQ wrote the paper.

ADDITIONAL INFORMATION

Competing interests: The authors declare that they have no competing interests.

REFERENCES

1. Scherz-Shouval R, Elazar Z. Regulation of autophagy by ROS: physiology and pathology. *Trends Biochem Sci.* 2011;36:30–8.
2. Sabharwal SS, Schumacker PT. Mitochondrial ROS in cancer: initiators, amplifiers or an Achilles' heel? *Nat Rev Cancer.* 2014;14:709–21.
3. Moloney JN, Cotter TG. ROS signalling in the biology of cancer. *Semin Cell Dev Biol.* 2017. <https://doi.org/10.1016/j.semcdb.2017.05.023>. pii: S1084-9521(16)30383-4.
4. He C, Klionsky DJ. Regulation mechanisms and signaling pathways of autophagy. *Annu Rev Genet.* 2009;43:67–93.
5. Mizushima N, Komatsu M. Autophagy: renovation of cells and tissues. *Cell.* 2011;147:728–41.
6. Kroemer G, Marino G, Levine B. Autophagy and the integrated stress response. *Mol Cell.* 2010;40:280–93.
7. Zhang L, Wang K, Lei Y, Li Q, Nice EC, Huang C. Redox signaling: potential arbitrator of autophagy and apoptosis in therapeutic response. *Free Radic Biol Med.* 2015;89:452–65.
8. Ni Z, Wang B, Dai X, Ding W, Yang T, Li X, et al. HCC cells with high levels of Bcl-2 are resistant to ABT-737 via activation of the ROS-JNK-autophagy pathway. *Free Radic Biol Med.* 2014;70:194–203.
9. Dewaele M, Maes H, Agostinis P. ROS-mediated mechanisms of autophagy stimulation and their relevance in cancer therapy. *Autophagy.* 2010;6:838–54.
10. Scherz-Shouval R, Shvets E, Fass E, Shorer H, Gil L, Elazar Z. Reactive oxygen species are essential for autophagy and specifically regulate the activity of Atg4. *EMBO J.* 2007;26:1749–60.
11. Schneider JG, Finck BN, Ren J, Standley KN, Takagi M, Maclean KH, et al. ATM-dependent suppression of stress signaling reduces vascular disease in metabolic syndrome. *Cell Metab.* 2006;4:377–89.
12. Guo Z, Kozlov S, Lavin MF, Person MD, Paull TT. ATM activation by oxidative stress. *Science.* 2010;330:517–21.
13. Alexander A, Cai SL, Kim J, Nanez A, Sahin M, MacLean KH, et al. ATM signals to TSC2 in the cytoplasm to regulate mTORC1 in response to ROS. *Proc Natl Acad Sci USA.* 2010;107:4153–8.
14. Zhang J, Tripathi DN, Jing J, Alexander A, Kim J, Powell RT, et al. ATM functions at the peroxisome to induce pexophagy in response to ROS. *Nat Cell Biol.* 2015;17:1259–69.

15. Zhang D, Wang W, Sun X, Xu D, Wang C, Zhang Q, et al. AMPK regulates autophagy by phosphorylating BECN1 at threonine 388. *Autophagy*. 2016;12:1447–59.
16. Kim J, Kundu M, Viollet B, Guan KL. AMPK and mTOR regulate autophagy through direct phosphorylation of Ulk1. *Nat Cell Biol*. 2011;13:132–41.
17. Sirtori CR. Aescin: pharmacology, pharmacokinetics and therapeutic profile. *Pharmacol Res*. 2001;44:183–93.
18. Patlolla JM, Raju J, Swamy MV, Rao CV. Beta-escin inhibits colonic aberrant crypt foci formation in rats and regulates the cell cycle growth by inducing p21(waf1/cip1) in colon cancer cells. *Mol Cancer Ther*. 2006;5:1459–66.
19. Yuan SY, Cheng CL, Wang SS, Ho HC, Chiu KY, Chen CS, et al. Escin induces apoptosis in human renal cancer cells through G2/M arrest and reactive oxygen species-modulated mitochondrial pathways. *Oncol Rep*. 2017;37:1002–10.
20. Tan SM, Li F, Rajendran P, Kumar AP, Hui KM, Sethi G. Identification of beta-escin as a novel inhibitor of signal transducer and activator of transcription 3/Janus-activated kinase 2 signaling pathway that suppresses proliferation and induces apoptosis in human hepatocellular carcinoma cells. *J Pharmacol Exp Ther*. 2010;334:285–93.
21. Ji DB, Xu B, Liu JT, Ran FX, Cui JR. beta-Escin sodium inhibits inducible nitric oxide synthase expression via downregulation of the JAK/STAT pathway in A549 cells. *Mol Carcinog*. 2011;50:945–60.
22. Zhu J, Yu W, Liu B, Wang Y, Shao J, Wang J, et al. Escin induces caspase-dependent apoptosis and autophagy through the ROS/p38 MAPK signalling pathway in human osteosarcoma cells in vitro and in vivo. *Cell Death Dis*. 2017;8:e3113.
23. Xie JM, Li B, Yu HP, Gao QG, Li W, Wu HR, et al. TIGAR has a dual role in cancer cell survival through regulating apoptosis and autophagy. *Cancer Res*. 2014;74:5127–38.
24. Galluzzi L, Pietrocola F, Levine B, Kroemer G. Metabolic control of autophagy. *Cell*. 2014;159:1263–76.
25. Chauhan S, Goodwin JG, Chauhan S, Manyam G, Wang J, Kamat AM, et al. ZKSCAN3 is a master transcriptional repressor of autophagy. *Mol Cell*. 2013;50:16–28.
26. Guo JY, Xia B, White E. Autophagy-mediated tumor promotion. *Cell*. 2013;155:1216–9.
27. Seglen PO, Gordon PB. 3-Methyladenine: specific inhibitor of autophagic/lysosomal protein degradation in isolated rat hepatocytes. *Proc Natl Acad Sci USA*. 1982;79:1889–92.
28. Mojzisova G, Kello M, Pilatova M, Tomeckova V, Vaskova J, Vasko L, et al. Anti-proliferative effect of beta-escin-an in vitro study. *Acta Biochim Pol*. 2016;63:79–87.
29. Prasad S, Gupta SC, Tyagi AK. Reactive oxygen species (ROS) and cancer: role of antioxidative nutraceuticals. *Cancer Lett*. 2017;387:95–105.
30. Galadari S, Rahman A, Pallichankandy S, Thayyullathil F. Reactive oxygen species and cancer paradox: to promote or to suppress? *Free Radic Biol Med*. 2017;104:144–64.
31. Cheng P, Kuang F, Ju G. Aescin reduces oxidative stress and provides neuro-protection in experimental traumatic spinal cord injury. *Free Radic Biol Med*. 2016;99:405–17.
32. Harikumar KB, Sung B, Pandey MK, Guha S, Krishnan S, Aggarwal BB. Escin, a pentacyclic triterpene, chemosensitizes human tumor cells through inhibition of nuclear factor-kappaB signaling pathway. *Mol Pharmacol*. 2010;77:818–27.
33. Qanungo S, Wang M, Nieminen AL. N-Acetyl-L-cysteine enhances apoptosis through inhibition of nuclear factor-kappaB in hypoxic murine embryonic fibroblasts. *J Biol Chem*. 2004;279:50455–64.